

# A Novel Direction for Non-Invasive Diabetes Prediction: Integrating Unani Wisdom with Sensor Technology

Sahar Waqar<sup>1†</sup>, Samyan Qayyum<sup>2</sup>, Talha Waheed<sup>2</sup>, Ahmed Shahid<sup>1</sup>, Amna Munir<sup>1</sup>, Anam Mukhtar<sup>1</sup>, and Rimsha Shahzad<sup>2</sup>, Non-members

## ABSTRACT

This study aims to modernize disease diagnosis in Unani medicine by utilizing signal processing techniques. Various features such as systolic and diastolic peaks, peak-to-peak interval, augmentation, and stiffness index were extracted from the pulse signals. These features were then used to train predictive models, including KNN, J48, and Random Forest. Predictive models achieved high precision rates: 100% for KNN, 99.2% for J48, and 94.3% for Random Forest, as evaluated through cross-validation. Integration of signal processing with traditional medicine holds potential to enhance diagnostic precision and alleviate healthcare burdens, offering a pathway for synergistic advancements in healthcare systems. Implementation of signal processing techniques in Unani medicine could streamline disease diagnosis, leading to more effective patient management and healthcare resource allocation. Integrating modern diagnostics with traditional medicine practices may foster greater acceptance and accessibility of alternative healthcare approaches, promoting holistic wellbeing within communities. This study pioneers the application of signal processing methods to pulse signals within Unani medicine, offering a novel approach to enhance disease diagnosis and advance traditional medical systems.

**Keywords:** Disease prediction using pulse, Unani Medicine, Diabetes prediction using non-invasive sensor, Health monitoring technology, Non-invasive diagnostic methods

## 1. INTRODUCTION

Information about human pulse signals can be used for disease diagnosis [1]. Ancient literature such as Unani Medicine (UM) [2], Traditional Chinese Medicine (TCM) [3], Ayurveda [4], and Siddha [5] used pulse signals to

diagnose patient health status. Unani Tibb/Medicine was introduced by Muslims approximately 1000 years ago by Hakim Ibn Sina (Avicenna) in 980 CE in Persia [6] which was later improvised and amalgamated with Arab, Turkish, and Iranian medicines. It is still practiced in the Middle East, South Africa and England [6].

In the Unani literature, the pulse is sensed at the radial artery on the wrist below the thumb by placing the middle, index, and ring fingers. The middle finger is placed on the median of the wrist, the ring finger is placed on the carpal, and the index finger is used to sense the cubit [7].

Pressure is exerted using three fingers on the artery to detect the pulse response. The main difference between the Unani literature and TCM is the placement of the finger to sense the pulse; Unani practitioners place the index finger closest to the heart, whereas TCM practitioners place the ring finger closest to the heart. The index finger is used for the compression, the middle finger is used for assessing the pulse rate, and the ring finger informs the condition of the vessel wall. The parameters considered for pulse diagnosis in the Unani literature are speed, force depth, and width [8]. There are seven points in the human body from which the pulse can be sensed; radial artery, temporal artery (side of the forehead), brachial artery (elbow), carotid artery (neck), femoral artery (upper thigh), popliteal artery (behind the knee) and dorsalis artery (top of thumb of foot) [9]. Any of these can be used to assess the patients.

According to hakims (physicians) who practice the Unani literature, there are two types of vessels that carry blood to the heart and other vessels that carry blood from the heart to other organs [8]. There are four phases in the pulse cycle: two movements (contraction/systole) and two pauses (relaxation/diastole). In systole, blood is pumped out of the heart, and in diastole, blood is pumped into the heart. Fig. 1 shows the key points of the pulse wave which are as follows: (a) represents the time taken for the contraction of the heart; (b) shows the time taken to relax the heart; (c) shows the external pause; (d) represents the gap between two successive pulse beats; and (e) shows the time taken for one complete pulse cycle, which is approximately equal to 0.8 seconds. Additional features can be computed using the derivative of the signal (A) of Fig. 1. When the function is increasing, then its derivative is positive, as shown in the Fig. 1 (signal B).

Manuscript received on August 12, 2024; revised on June 30, 2025; accepted on October 4, 2025. This paper was recommended by Associate Editor Krit Angkeaw.

<sup>1</sup>The authors are with Department of Civil Engineering, University of Engineering and Technology, Lahore, Pakistan.

<sup>2</sup>The authors are with the authors are with Department of Computer Science, University of Engineering and Technology, Lahore, Pakistan.

<sup>†</sup>Corresponding author: sahar.waqar@uet.edu.pk

©2025 Author(s). This work is licensed under a Creative Commons Attribution-NonCommercial-NoDerivs 4.0 License. To view a copy of this license visit: <https://creativecommons.org/licenses/by-nc-nd/4.0/>.

Digital Object Identifier: 10.37936/ecti-ec.2525233.255146

When signal (A) reaches a constant value, its derivative is 0. Subsequently, when the function (signal A) starts to decrease, the derivative is negative. When signal A reaches a constant value, the derivative becomes zero, and this process continues cyclically.  $\Delta T$  refers to the difference in time between the derivative of the systolic and diastolic peaks.

Pulse movement is evaluated based on its location and orientation. These pulsations indicate the health status of the human body. For example, a pulse with a large amplitude may indicate fever or inflammation in organs[8]. This art requires several years of practice. As this work is tedious and delicate, a computerized approach is developed to minimize human error.

Diabetes affects blood volume due to the presence of sugar content in the blood stream which damages vital organs [10]. It affects the elasticity of arterial walls and increases their stiffness. More clogged arteries(atherosclerosis) indicate that faster blood flow affects the pulse signal[11]. In UM, the circulation of blood flow and changes in blood volume with the application of pressure is detected using the fingers [12], which gives an indication of diabetes. This may be further verified by the practitioner using the urine test (attracting certain animals), physical symptoms (excessive thirst and frequent urination), etc. In this work, the machine learning based pulse diagnosis system is implemented by evaluating the pulse signal detected at the radial artery using the sensors. The proposed system is capable of recognising patients with compromised blood flow (Diabetic) with an accuracy of 100% with the k-Nearest-Neighbour (kNN) classifier, 99.2% with J48 and 94.3% with Random Forest (RF). This system will help develop a standardised approach to improve preparedness, response, and decision making capabilities, even in medical emergencies. It can also help intriage situations where time is the crucial factor. Non-invasive diagnosis can speed up the process considerably.

However, there are a few limitations; at the time of pulse examination, the patient should ideally have neither an empty nor a full stomach. The patient should have not exercised or exerted himself immediately prior to pulse examination. The pressure applied to the artery should be in proportion to the strength of the pulse. The pulse should be examined for at least thirty pulse cycles. All these factors can affect the pulse measurement quality and the disease diagnosis.

## 2. RELATED WORK

Pulse acquisition and disease diagnosis are primary areas of interest for several practitioners. Kim et al. studied pulse acquisition and diagnostic techniques. After signal acquisition using piezoelectric sensors, feature extraction is performed using wavelet transform, fast Fourier transform (FFT), and neurofuzzy analysis. This study also highlights that stroke, hypertension, arrhythmias, respiratory problems, diabetes, and thyroid problems are clinical diseases related to pulse signals[13].

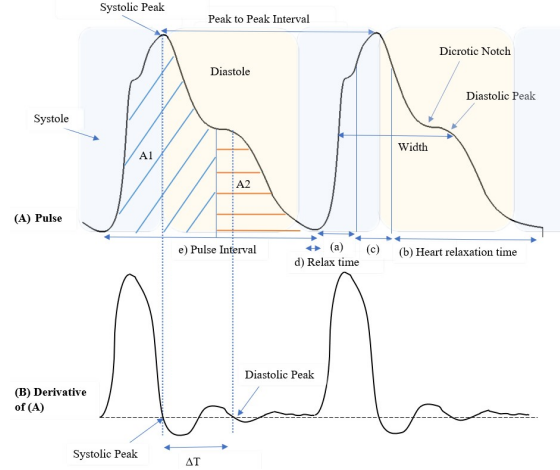


**Fig. 1:** Work flow of proposed method.

The pulse was acquired using a microphone to capture a low sound frequency with a low cut-off frequency of 12Hz. After frequency and time domain analysis, the features are extracted using autocorrelation followed by FFT. Support Vector Machine (SVM) was used for the classification of pre-meal and post-meal signals with accuracies of 88.8% and 81.48% respectively[14]. Similarly, [15] used a pressure sensor (350mm Hg), sampled at 500Hz, filtered with a low-pass filter. They extracted the rate-force rhythm, volume contact pressure, and pulse regularity. Dynamic time wrapping was used to classify the pulse according to its shape. In [16], an MLT-1010 piezoelectric sensor was used to sense a pulse followed by amplification. The QRS detection algorithm was used to calculate the pulse rate [17] [18] [19]. Polysomnography (PSG) and the 'energy ratio' have also been used to extract information from pulses [20]. [21], [22], [23], [24] used different features for pulse analysis through machine learning. In another approach, the wrist pulse signal was analyzed using a time-frequency distribution. After noise removal, the Gabor spectrogram was used for pulse analysis in the joint T-F space. Features such as the mean frequency, mean bandwidth, and time marginal integral are extracted. A low mean squared error was observed between the original and reconstructed signal[25]. Similarly, the pulse signal was compared to the ECG signal [26]. The complete pulse spectrum was obtained as a time series with no interference noise. The ten basic features of the pulse are frequency, pressure, depth, width, expansion quality, interlude quality, rhythm, regularity, definition, and tension [27] [28] [29] [30].

Basic and derived features can then be used for the diagnosis of diseases or to determine the correlation between the disease and pulse parameters. For example, [31] have used a Doppler ultrasound device to detect the pulse signal. After signal processing, a modified Gaussian model was proposed to extract useful features. Fuzzy C-means clustering was then used to classify the healthy and diseased subjects. In another study on

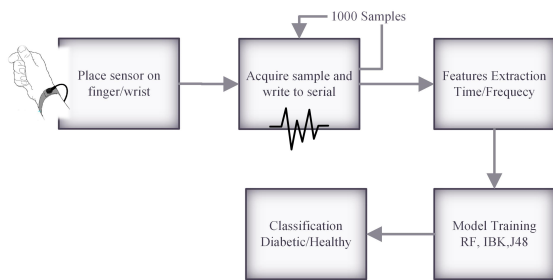


Fig. 2: The Methodology.

arterial pulse pressure propagation, the non-linear KdVe model was used on a preprocessed signal to extract features as a clinical approach for the identification of hypertensive states[32]. Similarly, lungs cancer detection was performed based on TCM principles[33]. In Ayurvedha medicine, the three pulses are called 'Tridosha', Vata, Pitta, and Kappa. The researchers in [34] used one piezoelectric sensor for signal acquisition and classified the diseases according to the values of 'Vata', 'Pitta' and 'Kappa'. Similarly, [35] used three pressure sensors to acquire the 'Tridosha' signal which was later amplified. The authors claimed that the system has the potential to diagnose obesity, asthma, cancer, hepatitis, etc. However, no validation was provided. The authors in [36] used a similar concept and classified 42 subjects into healthy and unhealthy classes with the help of the signal acquired using a piezoresistive sensor for five minutes with a sampling rate of 1000Hz. The classification was done using kNN, SVM, and linear discriminant analysis (LDA), etc. Additionally, [37] worked on the detection of cardiac-related diseases. [38] discussed possibility of the disease in the subject based on the imbalance in three main signals. From the literature, it has been observed that naturopaths are working hard to find their place in medicine due to disapproval at both the national and global levels. Some countries practice UM, TCM, etc. have access to local patients for the validation of their results. However, they also lack proper filing and documentation of patient health records as there are no adequate hospitals that support this type of medicine. It was also observed that there is limited English literature for UM. We carried out this study in renowned local hospitals in Lahore (LHR), i.e. Shalamar Hospital LHR, Ganga Ram Hospital LHR, and Mozang Hospital LHR Pakistan. We implemented our prototype in confirmed diabetic individuals with the approval of officials. In this way, we managed to validate our disease diagnosis results in a reasonable population with promising results..

### 3. METHODOLOGY

Two sensors are used to acquire the signal for further processing. The first one is the PPG while the second one is a piezoelectric sensor. Obtained signals are evaluated by the UM Physician.

#### 3.1 Pulse Signal Acquisition

Sensitive transducers such as piezoelectric sensors, piezoresistive sensors, ultrasonic sensors, optical sensors, and force-sensitive resistors are required to capture the pulse signal. In this work, the PPG and the piezoelectric sensor are used. We acquired 1000 signal samples applying pressure, extracted features, trained the model and performed the diagnosis using ML techniques as shown in Fig. 2.

#### 3.2 Sensor 1: The Pulse Oximeter

##### 3.2.1 Sensing Technique

Pulse (PPG) is sensed using red light whose frequency could be varied from 50Hz to 1000Hz. The LED current and pulse width could also be modified within a specific range that affected the intensity of light coming from the LED. Differences in skin tone and thickness require higher-intensity light to detect blood flow. The oximeter measures the light that is dispersed due to blood flow. The light is incident upon the skin through the LED, and the reflected light is captured in a photodetector. The photodetector output gave rise to a signal that is further processed. The connection diagram is illustrated in figure3. The sampling frequency of the PPG sensor is 50 Hz – 1000 Hz and the piezo sensor has a sampling rate of 200 kHz – 1 MHz. The PPG is sampled at  $f_s = 100$  Hz. A total of 500 samples are acquired for each patient.

##### 3.2.2 Signal Validation

The signal obtained from the oximeter is useful in calculation of blood oxygen levels and pulse rate, etc. The unani practitioner does not simply measure blood circulation. Although useful, this information was not enough to build a pulse diagnostic prototype. The practitioner must sense the physical movement of the artery in the wrist through the fingers. These features may include the basic pulse features as given in [27], which cannot be extracted with the oximeter.

#### 3.3 Sensor 2: The Piezoelectric Sensor

##### 3.3.1 Sensing Technique

Piezoelectric sensor senses the potential difference produced by pressing /squeezing the artery with the fingers. Certain crystals, ceramics, and even biological matter such as bone and DNA exhibit piezoelectricity. This sensor is useful as it could measure small pressure changes. Due to its passive nature, it did not have a heating problem and gave really accurate readings.

The pressure to be measured is applied to a thin metal plate. The total force on the plate is the product of the active area of the plate, which is the area within which the pressure is applied and the applied pressure. This force is mechanically transferred to the crystal [39] [40]. The stress applied to the crystal gave rise to a potential difference, which resulted in a current flow. When placed at the radial artery, its movement caused

**Table 1:** Specifications and Calibration Summary of the Custom Sensor System.

Parameter	Description
Sensor Type	Non-invasive, pulse waveform sensor (radial)
Additional Measurements	Skin temperature, skin conductivity
Sampling Rate	200 Hz
Sensor Calibration Method	Manual calibration using reference waveforms
Calibration Tool	Clinical pulse reading by Unani practitioners
Signal Consistency (Same subject, repeated 3 times)	more than 95% waveform overlap
Signal Drift	less than 3% over 10 minutes
Noise Filtering	Low-pass Butterworth filter (cutoff = 5 Hz)
Power Supply	5V (USB-powered)
Data Interface	USB Serialh
Form Factor	Wrist-mountable prototype

a varying pressure on the sensor, and thus a varying voltage is generated which is termed as the pulse signal.

Table 1 summarizes the specifications and calibration results of the self-developed pulse sensor system. To ensure measurement accuracy, calibration was performed using expert-assessed clinical readings from Unani practitioners. The system demonstrated over 95% repeatability across three consecutive trials on the same subjects, with minimal drift over short time periods. These results support the reliability of the sensor system in capturing consistent physiological signals necessary for diabetes classification.

### 3.3.2 Signal Validation

The proposed sensor system was custom-built to non-invasively capture pulse signals from the radial artery, inspired by diagnostic practices in Unani medicine. The hardware was designed to record pulse waveforms and basic physiological signals such as temperature and conductivity. Accuracy was ensured through repeated measurements, and the system's outputs were compared against standard pulse assessments by Unani practitioners. Preliminary tests indicated that the sensor exhibited consistent waveform patterns for the same subject under similar conditions, with minimal signal drift. Although this is a prototype-stage system, it has demonstrated adequate reliability to support the exploratory nature of this research. Future versions of the system will include enhanced signal resolution and clinical benchmarking to validate sensor accuracy against medical-grade equipment. Furthermore, the literature [16], [41], [31], [13], [34] also proved the usefulness of the sensor.

### 3.4 Signal Storage

The sensors are interfaced with the Arduino UNO through its I 2C pins and transmitted to the computer through the serial port. The received signal is saved as a vector in MATLAB, and the workspace is exported as

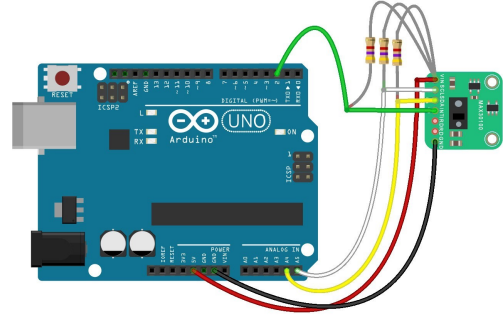


**Fig. 3:** The Schematic for the Oximeter Connection with Arduino UNO.

a mat file. The features extracted from the signal were saved in a relational database SQL Server.

### 3.5 The Dataset of Diabetic and Healthy Patients

The data set of diabetic patients is collected from Shalamar Hospital, Services, Ganga Ram and Mozang Hospitals in Lahore. Signals from the 18 patients are recorded using a piezoelectric sensor. Samples of profiles are shown in Tab. 2. Pulse is taken for both male and female patients. There are 12 female and 6 male subjects. Information about their height, age, weight, body mass index, and gender is also recorded to extract features of the signal. The average age of the male patients is 63 while that of the female patients is 57. Similarly, dataset of healthy patients is collected from students of UET, Lahore. 22 samples were taken, of which some profiles are shown in the Tab. 3. The signal is recorded from 6 male students and 14 female students. The same parameters as in Table 2 are recorded. The average age of the healthy female subject is 21 years, and the average age of the healthy male subject is 22 years.

### 3.6 Extracted Features

The pulse signal has two phases:

- Anacrotic phase: the rising edge.
- Catacrotic phase: the falling edge.

High blood sugar affects vital organs, especially the heart. Therefore, a diabetic patient is expected to have a composed blood flow, heart, and circulation system. The following features are extracted from the signal. They are physiologically important in the prediction of diabetes, as they help to understand the current status of the heart.

**Augmentation Index (AI):** It is the measure of arterial thickness calculated by dividing augmentation pressure ( $y$ ) by the pulse pressure ( $x$ ) as shown in Eq. (1). The wave reflected from the periphery to the centre is used to measure systolic arterial pressure [42]. It measures the arterial stiffness and increases with age.

$$AI = \frac{y}{x} \quad (1)$$

**Dicrotic Notch (DN):** The center between the systolic

**Table 2: The Profile of the Diabetic Subjects.**

No	Gender	Age	Weight (kg)	Height	BMI	Category
1.	Male	45	70	5'8"	23.46	Diabetes
2.	Male	60	50	5'2"	20.16	Diabetes
3.	Female	58	58	5'2"	23.38	Diabetes
4.	Male	58	95	5'8"	31.84	Diabetes
5.	Male	65	128	6'3"	35.27	Diabetes
Mean Age = 60, Mean Weight = 85, Mean Height = 5'5", Mean BMI = 25.23						

**Table 3: The Profile of the Healthy Subjects.**

No	Gender	Age	Weight (kg)	Height	BMI	Category
1.	Female	22	47	5'4"	17.78	Healthy
2.	Female	21	37	5'3"	14.44	Healthy
3.	Female	22	45	5'4"	17.01	Healthy
4.	Male	24	67	5'6"	23.84	Healthy
5.	Female	22	50	5'5"	18.34	Healthy
Mean Age = 60, Mean Weight = 85, Mean Height = 5'5", Mean BMI = 19.25						

and the diastolic peak is another peak which is known as the dicrotic notch (DN) [43]. It arises because of the closing of the aorta valve. The change in its shape or position can be caused by arterial wave pressure [44]. DN is indicative of Systemic Vascular Resistance (SVR) which is the resistance in the circulatory system. High DN implies high SVR.

**Stiffness Index (SI):** The systolic component of the pulse signal comes from a forward pressure wave transmitted along a direct path from the left ventricle to the finger. SI is a measure of arterial dispensability and is used to find age-related problems such as arterial stiffness. The SI is calculated from the body height ( $h$ ) divided by the time delay between the pulse systolic peak and the inflection point of the reflected wave ( $\Delta T$ ) as given in Eq. (2).

$$SI = \frac{h}{\Delta T} \quad (2)$$

**Peak to Peak Interval (P2P):** It is the time interval between the two consecutive systolic peaks as given in Eq. (3) and used to calculate no of heartbeats in a minute. Diabetes or high blood sugar levels are associated with high heart rate [45].

$$P2P = \frac{\text{samplingrate}}{\text{peak}(i+1) - \text{peak}(i)} \quad (3)$$

**Systolic Peak (SP):** It is the pointer of pulsatile changes in the blood volume produced by the blood flow. Low SP is indicative of the high arterial blood pressure which means low blood volume pulsation in arteries. Conversely, high SP means low arterial blood pressure meaning high blood volume pulsation in the arteries. The SP is inversely proportional to the systolic pressure. Young people have elastic arteries and they harden over time. This reduces arterial resistance which reduces arterial capacitance. As a consequence, arterial blood

volume falls which causes a low SP [46].

**Diastolic Peak (DP):** It is caused by reflected waves from arteries of the lower body [47].

$\Delta T$  : The peak-to-peak time taken for blood to move from the heart to the periphery and back. The time between the systolic and diastolic peaks is  $\Delta T$ . It is defined as the time between the waveform peak and the dicrotic notch on the down slope of the waveform which is a local maximum of the first derivative.

**Pulse Width (PW):** It is a measure of how long it takes for the complete systolic and diastolic cycle to complete.

**Infection Point Area (IPA):** It is the total area under the pulse signal curve.  $A1$  and  $A2$  are the areas under the signal separated at the DN. The IPA ratio can be calculated by dividing  $A2$  by  $A1$  as given in Eq. (4). It is a predictive factor of adverse cardiac events.

$$IPA = \frac{A2}{A1} \quad (4)$$

### 3.7 The Classifier/Diagnosis and the Visualization

The pulse of several diabetic patients had the following appearance as shown in Fig. 4. It was observed that the dicrotic notch for the diabetic patients has different magnitude than the healthy ones. Three different supervised algorithms are used for classification using the signal set ( $X$ ) and the feature set ( $Y$ ) as given in Eqs. (5) and (6). Dataset is divided into train and test set. Training is performed on the classified group  $X$  using a set of extracted features, that is,  $Y$ .

$$X = \text{signal1}; \text{signal2}; \dots \quad (5)$$

$$Y = \text{features1}; \text{features2}; \dots \quad (6)$$

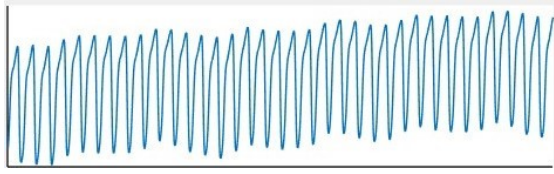


**Fig. 4: The Pulse of a Diabetic Patient.**

A Graphical User Interface (GUI) is also developed for visualisation that has the options for starting, stopping, re-updating and store the desired tasks. The signal takes time to settle due to noise. When it stabilises, the signal is saved.

## 4. RESULTS

### 4.1 The Validity of the Pulse Signal using ECG

To understand our extracted signal, we have studied two datasets [48] and [49]. Dataset1 contained 53 samples of the lead II ECG signal and its frequency, PPG signal, age, weight, SPO2, heart and respiratory signal, etc. which was used in [50] to estimate the respiratory rate (RR) from the pulse signals. Similarly, data set2 contained 42 samples of eight-minute-long raw PPG signal, labelled pulse peak and artefacts, reference CO2 signal, ECG signal, instantaneous RR, heart rate (HR) and the output of algorithms. The ECG signal is compared with the raw PPG signal to find similarities between the two. It was found that both signals can determine HR. If both are measured simultaneously, both can determine the pulse transit time (PTT). The distance between the R peak of the ECG and the maximum slope of the PPG is the same and is found to be the PTT which could be used to measure systolic blood pressure. PPG and ECG signals contain their own diagnostic information. This is used to calculate the respiratory rate using three different features, namely the frequency, intensity, and amplitude of the PPG. An ECG wave consists of a PQRST wave as shown in Fig. 5. Atrial depolarisation is represented by a P wave. Ventricular depolarisation is indicated by the QRS wave, which consists of a Q wave, a R wave, and a S wave. This is used to monitor the activity of cardiac heart tissue. ECG provides physicians with a complete description of heart activity. The R peak is the largest spike in the ECG signal. When the blood exits, the R peak develops. The time interval between the R peak of the ECG and the maximum slope of the PPG is identical and is called the PTT. It involves the simultaneous measurement of the pulse signal and the ECG. Researchers have tried to estimate the systolic blood pressure of PTT. To understand the difference between PPG and ECG, the information is summarised in Fig 5. Both signals contain diagnostic information related to cardiac activity, i.e. HR and morphology, etc. The former is sensed using the photo-diode sensor, while the latter is sensed using the electrodes.

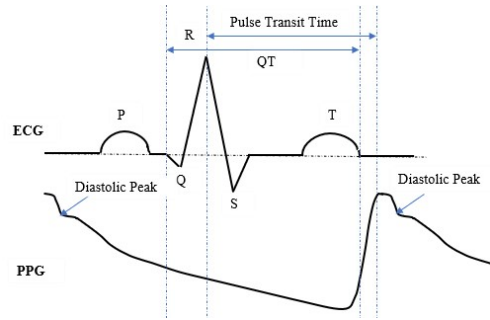


**Fig. 5: The ECG Complex.**

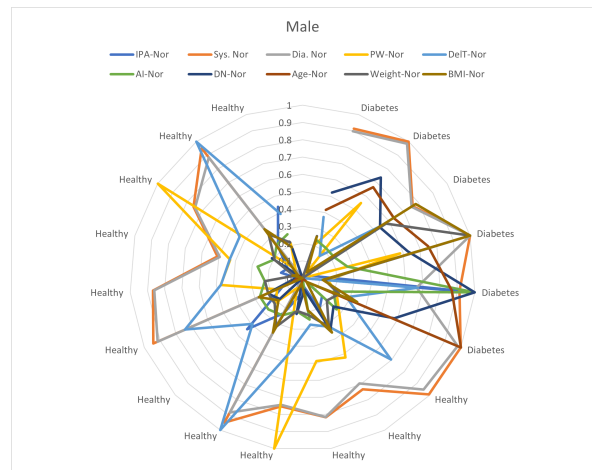


**Fig. 6: The Pulse Profile of the Male Diabetic and Healthy Patients.**

### 4.2 The Results from the Collected Dataset

#### 4.2.1 Pulse Profile of the Diabetic and Healthy Subjects

It is observed that the variation of the dicrotic notch indicates that a person has diabetes. The actual dicrotic notch can be compared with the diseased pulse. The calculated dicrotic notch for patients with diabetes is found to be high, as can be seen in the Tab. 4. For better understanding, a comparative analysis is performed on male and female diabetic and healthy patients separately. Figs. 6 and 7 shows the radar graph of male and female subjects respectively. All features are normalized to allow for a better comparison to be illustrated. The DN in both figures is higher in diabetic patients ( $> 0.5$ ) than the healthy subjects. All other attributes are found to be in the same range for both the diabetic and healthy subjects. However, the accumulation of all the desired features are in higher region in diabetic patients for both males and females. Detailed analysis of characteristics has been shown in Table 5 where the mean and standard deviation are calculated separately for both male and female subjects for the diseased and healthy class.

#### 4.2.2 Machine Learning Models

We have used three different machine learning algorithms and trained the model. We found that all of them

**Table 4:** Features Extracted from Collected Dataset.

ID	Disease	IPA	Avg. Systolic	Avg. Diastolic	Pulse Width	$\Delta T$	A.I.	DN
1.	Diabetes	0.99	942	926	22.13	2.05	1.017	0.0275
2.	Diabetes	1.01	1023	1008	58.97	1.5	1.01	0.0361
3.	Diabetes	1.21	647	526	20.75	3.5	1.23	0.0307
4.	Diabetes	0.99	801	790	1.36	2.6	1.01	0.028
5.	Diabetes	1	1023	1022	62.31	1.08	1.03	0.0317
6.	Diabetes	1.12	934	851	61.32	2.23	1.00	0.0261
7.	Diabetes	1.47	429	363	65.4	1.9	1.18	0.0286
8.	Diabetes	1.37	940	704	16.72	2.82	1.33	0.0467
9.	Diabetes	0.98	1023	1003	23.82	1.80	1.00	0.0298
..	..	..	..	..	..	..	..	..
31.	Healthy	1.04	1008.06	769.12	29.64	3.86	0.99	0.0095
32.	Healthy	1.04	1017.63	977.04	31.38	2.89	1.03	0.0162
33.	Healthy	1.06	773.40	733.04	56.13	1.91	0.92	0.0201
34.	Healthy	1.00	852.40	848.36	52.34	1.79	1.02	0.0092
35.	Healthy	1.02	645.05	627.27	39.38	2.79	1.03	0.0090

A.I. refers to Augmentation Index, DN refers to Dicrotic Notch

**Table 5:** Statistical Information on the Extracted Features.

Sex	Type	MR	IPA	Avg. Sys	Avg. Dia	Pulse Width	$\Delta T$	A.I.	DN
M	DB	Mean	1.06	958.67	908.83	30.89	1.98	1.07	0.03
M	DB	$\sigma$	0.15	87.06	132.58	24.39	0.66	0.13	0.01
M	HT	Mean	1.05	733.31	706.85	44.25	2.51	1.01	0.01
M	HT	$\sigma$	0.05	324.51	314.89	33.34	0.65	0.03	0.005
F	DB	Mean	1.12	811.2	714.13	41.45	2.63	1.13	0.03
F	DB	$\sigma$	0.26	263.55	258.24	21.11	0.91	0.1	0.003
F	HT	Mean	1.02	750.7	715.12	39.77	2.6	1	0.01
F	HT	$\sigma$	0.03	214.66	200.03	18.32	0.54	0.04	0.003

F refers to Female, M = Male, DB = Diabetes, HT = Healthy, MR = Measure, Sys = Systole, Dia = Diastole

**Table 6:** Results of Applied Classifiers.

Algorithm	RAE (%)	ACC(%)	PRE	TP	FP	FN	TN
J48	14.6322	99.2346	0.992	9	0	2	24
RF	0.2926	94.2857	0.943	9	0	0	26
kNN	7.45	100	1.0	9	0	0	26

TP = True Positive, TN = True Negative, FP = False Positive, FN = False Negative, and RAE refers to Relative Absolute Error

performed quite well with KNN being on top with 100% accuracy and precision equal to 1.0. Results from these classifiers are shown in the table 5 where a means diabetic and b means healthy.

Compared with the existing work[36], where KNN, SVM and LDA are used, novelty of our work is to apply and compare the classification algorithms on the data produced based on the theory of Unani Medicine Practitioners. J48 algorithm was used to generate a decision tree in WEKA which selected the best attributes for classification. In this algorithm, pruning was performed to decrease classification errors produced by the training set. All continuous, discrete attributes and missing values in the training set were handled by the J48.

**Random Forest (RF)** can be used for classification and regression tasks in supervised learning. In this algorithm, multiple decision trees were formed. Randomness was added with the help of growing trees and good results were produced through its default hyper-parameters. However, it gave slow prediction.

**IBK** stands for instance based learner. We applied a KNN-algorithm on the dataset in WEKA. IBK had different variants which differed by the distance measuring technique e.g. euclidean, manhattan, and chebyshev etc. An appropriate value of k is selected through cross validation. For each test sample, distance was calculated to its nearest neighbors and based on the shortest distance, the class of the test sample was predicted.

#### 4.2.3 The Impact of Other Diseases on the Pulse

There can be certain cases where patients are suffering from more than one disease or another disease impacts the morphology of the pulse. For example, a person may suffer from atherosclerosis without diabetes or may have both. In that case, further tests can be used to confirm the diagnosis. However, as per the expert (tabib) if the blood sugar is sufficient enough to be detectable ( $> 200\text{mg/dl}$ ) by the pulse signal it implies that a person is either suffering from the diabetes or

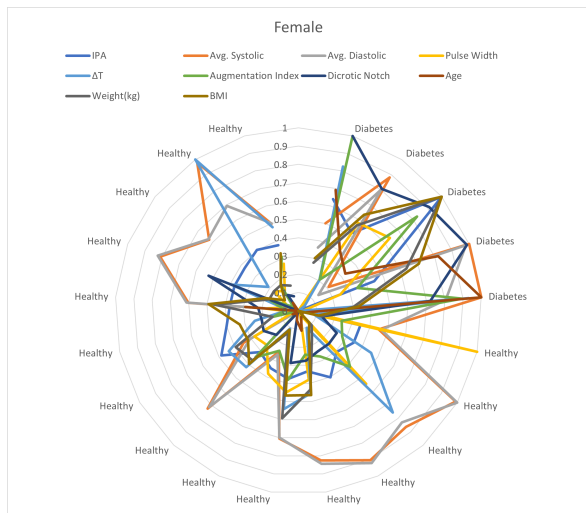


**Fig. 7:** The Pulse Profile of the Female Diabetic and Healthy Patients.

had eaten reasonable amount of sugar. The physiological features addresses the condition of the heart which is the aftermath of the damage caused by the diabetes. It is quite possible that an early diabetes (Type-1) may go unnoticed with the proposed technique. However, more data (type-1 confirmed cases) is required to confirm this hypothesis. Therefore, the tabi uses both the pulse features, physical symptoms, and other non-invasive techniques to address the ambiguity in the diagnosis. For generalization, the collected dataset also contains few patients with both heart disease and diabetes, or only diabetes.

## 5. CONCLUSION

In Unani medicine, most diseases can be diagnosed by detecting imbalance in the four humours of the human body. Pulse plays an important role as a measurable input for disease diagnosis. The literature showed hepatitis [20], pancreatitis [31], fever, constipation, flatulence [41], lung cancer [33], type 1 and type 2 hypertension [32], etc. could be diagnosed using the pulse.

Although the dataset used in this study is limited in size, it was sufficient for this feasibility-stage research. The data represents a unique combination of Unani pulse readings and non-invasive sensor measurements, which required domain experts and custom hardware for acquisition. To ensure meaningful results, we employed k-fold cross-validation and regularization techniques to avoid overfitting and enhance model robustness. The consistent patterns observed across samples indicate that the dataset, while modest, provides adequate support for the exploratory objectives of this study.

It is important to note that the diabetic subjects were, on average, older than the healthy controls. This is consistent with the typical onset patterns of type 2 diabetes, which is predominantly found in middle-aged and elderly populations. While this introduces age as

a potential confounding variable, the objective of this exploratory study was to identify biometric patterns related to diabetes irrespective of age. The limitation has been acknowledged, and future work will focus on age-matched cohorts to validate findings.

With this study, it is observed that the heritage of the Unani practitioners was purely scientific and could be modelled. The results are very encouraging and can be studied further to develop a comprehensive noninvasive disease diagnosis system for other diseases [20],[51],[26],[16],[31],[8] which can also save millions of dollars spent on healthcare care each year on laboratory tests. This study can also be extended by increasing the number of points for pulse acquisition. More features can be incorporated for better classification and also to increase the classes of diseases to be identified. The second derivative of the pulse waveform can give a measure of the pulse wave velocity. The Fourier and the Hilbert-Hauge transforms can be used to extract even more features from the pulse waveform and also to develop a higher understanding of the signal.

However, this knowledge is dying due to the shortage of literature in recent languages, the lack of documentation, the deaths of practitioners, and the lack of trust in medicine in the scientific community. The main purpose of this study was to initiate research in this domain. This prototype can serve as a stepping stone for anyone who wants to work on pulse diagnosis and cannot find the right place to begin with.

## DECLARATIONS

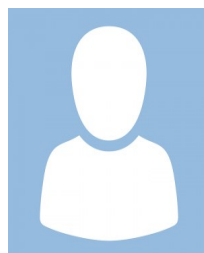
- Funding Statement: This research did not receive any external funding.
- Ethical Compliance: All procedures performed in studies involving human participants were in accordance with the ethical standards of the institutional and/or national research committee and with the Declaration of Helsinki of 1964 and its subsequent amendments or comparable ethical standards.
- Conflict of Interest declaration: The authors declare that they have no affiliations or involvement in any organisation or entity with any financial interest in the subject matter or materials discussed in this manuscript.

## REFERENCES

- [1] C. Guo, Z. Jiang, H. He, Y. Liao, and D. Zhang, "Wrist pulse signal acquisition and analysis for disease diagnosis: A review," *Computers in Biology and Medicine*, vol. 143, pp. 105–312, 2022.
- [2] F. Eram, M. A. Quamri, M. D. A. Bhat, U. Siddiqui, and S. Nida, "Perspective of ischemic heart disease (iqfari marad-i-qalb) with reference to unani medicine," *Bangladesh Journal of Medical Science*, vol. 22, no. 3, 2023.
- [3] X. Zhu, F. Wang, J. Mao, Y. Huang, P. Zhou, and J. Luo, "A protocol for digitalized collection of traditional chinese medicine (tcm) pulse infor-

- mation using bionic pulse diagnosis equipment,” *Phenomix*, vol. 3, no. 5, pp. 519–534, 2023.
- [4] M. Deshmukh and M. Khemchandani, “Illness diagnosis based on ayurveda (vat, pitta, kapha dosha) using machine learning,” in *2023 6th International Conference on Advances in Science and Technology (ICAST)*, pp. 213–216, IEEE, 2023.
- [5] S. Krishnan *et al.*, “IoT based siddha diagnosis for human health monitoring,” *Indian Journal of Traditional Knowledge (IJTK)*, vol. 22, no. 4, pp. 717–726, 2023.
- [6] C.-T. Che, V. George, T. Ijnu, P. Pushpangadan, and K. Andrae-Marobela, “Traditional medicine,” in *Pharmacognosy* (S. Badal and R. Delgoda, eds.), pp. 15–30, Elsevier, 2017.
- [7] G. Townsend and Y. De Donna, *Pulses and impulses: a practitioner’s guide to a unique new pulse diagnosis technique*. Thorsons, 1990.
- [8] M. Khazir, *Pulse: Let’s Understand and Practice (Its Description in Unani and Conventional Medicine)*. Educreation Publishing, 2017.
- [9] W. Stanley and L. Mark, “Human cardiovascular system,” *Encyclopædia Britannica*, 2024.
- [10] D. Mohajan and H. K. Mohajan, “Hyperglycaemia among diabetes patients: A preventive approach,” *Innovation in Science and Technology*, vol. 2, no. 6, pp. 27–33, 2023.
- [11] Y. K. Qawqzeh, A. S. Bajahzar, M. Jemmali, M. M. Otoom, A. Thaljaoui, *et al.*, “Classification of diabetes using photoplethysmogram (ppg) waveform analysis: logistic regression modeling,” *BioMed Research International*, vol. 2020, 2020.
- [12] S. Kumar, S. Kumar, and K. Veer, “Pulse (nadi) analysis for disease diagnosis: A detailed review,” *Proceedings of the National Academy of Sciences, India Section A: Physical Sciences*, vol. 93, no. 1, pp. 135–145, 2023.
- [13] S. Gan, Q. Zhuang, and B. Gong, “Humancomputer interaction based interface design of intelligent health detection using pcanet and multi-sensor information fusion,” *Computer Methods and Programs in Biomedicine*, vol. 216, p. 106637, 2022.
- [14] N. N. Khaire and Y. V. Joshi, “Diagnosis of disease using wrist pulse signal for classification of pre-meal and post-meal samples,” in *2015 International Conference on Industrial Instrumentation and Control (ICIC)*, pp. 866–869, IEEE, 2015.
- [15] N. Roopini and J. Shivaram, “Design & development of a system for nadi pariksha,” *Children*, vol. 1, p. 10, 2015.
- [16] C. Guo, Z. Jiang, H. He, Y. Liao, and D. Zhang, “Wrist pulse signal acquisition and analysis for disease diagnosis: A review,” *Computers in Biology and Medicine*, vol. 143, p. 105312, 2022.
- [17] S. K. Mathew and C. Jamuna, “Pulse sensor design for disease diagnosis,” *International Journal of Innovative Research and Development*, 2014.
- [18] C. Shah, R. Warkhedar, C. Ladekar, and S. Gandhi, “Fundamentals of nadi pariksha: A review of ancient ayurvedic holistic diagnostic tool,” in *AIP Conference Proceedings*, AIP Publishing, 2024.
- [19] M. Palakurthi, L. Fergusson, S. N. Dornala, and R. H. Schneider, “Diagnostic validity of ‘ayurvedic pulse assessment: Maharishi n̄adivigȳan in cardiovascular health,” *Journal of Maharishi Vedic Research Institute*, vol. 17, p. 33, 2021.
- [20] Z. Jiang, D. Zhang, and G. Lu, “A robust wrist pulse acquisition system based on multisensor collaboration and signal quality assessment,” *IEEE Transactions on Instrumentation and Measurement*, vol. 71, pp. 1–10, 2022.
- [21] C. Guo, Z. Jiang, and D. Zhang, “Multi-feature complementary learning for diabetes mellitus detection using pulse signals,” *IEEE Journal of Biomedical and Health Informatics*, vol. 26, no. 11, pp. 5684–5694, 2022.
- [22] P. Prasun, S. Mukhopadhyay, and R. Gupta, “Real-time multi-class signal quality assessment of photoplethysmography using machine learning technique,” *Measurement Science and Technology*, vol. 33, no. 1, p. 015701, 2021.
- [23] J. Chen, K. Sun, R. Zheng, Y. Sun, H. Yang, Y. Zhong, and X. Li, “Three-dimensional arterial pulse signal acquisition in time domain using flexible pressure-sensor dense arrays,” *Micromachines*, vol. 12, no. 5, p. 569, 2021.
- [24] Q. Zhang, J. Zhou, and B. Zhang, “Graph based multichannel feature fusion for wrist pulse diagnosis,” *IEEE Journal of Biomedical and Health Informatics*, vol. 25, no. 10, pp. 3732–3743, 2020.
- [25] N. Garg and N. Babbar, “Feature extraction of wrist pulse signals using gabor spectrogram,” *Indian Journal of Science and Technology*, vol. 9, no. 47, pp. 1–8, 2016.
- [26] Z.-D. Liu, J.-K. Liu, B. Wen, Q.-Y. He, Y. Li, and F. Miao, “Cuffless blood pressure estimation using pressure pulse wave signals,” *Sensors*, vol. 18, no. 12, p. 4227, 2018.
- [27] S.-C. Tang, P.-W. Huang, C.-S. Hung, S.-M. Shan, Y.-H. Lin, J.-S. Shieh, D.-M. Lai, A.Y. Wu, and J.-S. Jeng, “Identification of atrial fibrillation by quantitative analyses of fingertip photoplethysmogram,” *Scientific Reports*, vol. 7, no. 1, pp. 1–7, 2017.
- [28] C. Fuster-Barcel’o, A. Guerrero-L’opez, C. Camara, and P. Peris-Lopez, “Exploring the power of photoplethysmogram matrix for atrial fibrillation detection with integrated explainability,” *Engineering Applications of Artificial Intelligence*, vol. 133, p. 108325, 2024.
- [29] D. Pachori, R. K. Tripathy, and T. K. Jain, “Detection of atrial fibrillation from ppg sensor data using variational mode decomposition,” *IEEE Sensors Letters*, vol. 8, 2024.
- [30] M. M. Bassiouni, S. A. Gouda, M. A. Abdalgelel, H. A. Elbadry, O. A. Mohamed, N. A. Mahmoud, A. R. Mousa, and E.-S. A. El-Dahshan, “Mobile

- application for heart diseases diagnosis based on the ppg signals and deep learning,” in *2023 Eleventh International Conference on Intelligent Computing and Information Systems (ICICIS)*, pp. 403–410, IEEE, 2023.
- [31] Y. Chen, L. Zhang, D. Zhang, and D. Zhang, “Wrist pulse signal diagnosis using modified gaussian models and fuzzy c-means classification,” *Medical Engineering & Physics*, vol. 31, no. 10, pp. 1283–1289, 2009.
- [32] M. R. Alfonso, R. L. Armentano, L. J. Cymberknop, A. R. Ghigo, F. M. Pessana, W. E. Legnani, *et al.*, “A novel interpretation for arterial pulse pressure amplification in health and disease,” *Journal of Healthcare Engineering*, vol. 2018, p. 1364185, 2018.
- [33] Z. Zhang, A. Umek, and A. Kos, “Computerized radial artery pulse signal classification for lung cancer detection,” *Facta Universitatis, Series: Mechanical Engineering*, vol. 15, no. 3, pp. 535–543, 2017.
- [34] S. K. Mathew and C. Jamuna, “Pulse sensor design for disease diagnosis,” *International Journal of Innovative Research and Development*, 2014.
- [35] S. P. Sharoni Narang, O. Batwal, and M. Khandagale, “Ayurveda based disease diagnosis using machine learning,” *International Research Journal of Engineering and Technology*, vol. 5, no. 3, pp. 3704–7, 2018.
- [36] K. Goyal and R. Agarwal, “Pulse based sensor design for wrist pulse signal analysis and health diagnosis,” *Biomed. Res.*, vol. 28, no. 12, pp. 5187–5195, 2017.
- [37] R. V. Shinde and M. S. Patil, “Diagnosis of disease using wrist pulse signals,” *JournalNX*, pp. 233–236, 2018.
- [38] D. Gaddam *et al.*, “A survey on nadi pareeksha for early detection of several diseases & computational models using nadi patterns,” *International Journal of Computer Science and Information Technologies*, vol. 6, no. 4, pp. 3424–3425, 2015.
- [39] M. Farooq and E. Sazonov, “Segmentation and characterization of chewing bouts by monitoring temporalis muscle using smart glasses with piezoelectric sensor,” *IEEE Journal of Biomedical and Health Informatics*, vol. 21, no. 6, pp. 1495–1503, 2016.
- [40] B. M. Bell, R. Alam, N. Alshurafa, E. Thomaz, A. S. Mondol, K. de la Haye, J. A. Stankovic, J. Lach, and D. Spruijt-Metz, “Automatic, wearable-based, in-field eating detection approaches for public health research: a scoping review,” *NPJ Digital Medicine*, vol. 3, no. 1, p. 38, 2020.
- [41] S. Kumar, K. Veer, and S. Kumar, “Development of an adjustable pulse measurement system for determining the precise position for recording high wrist pulse signals,” *Mapan*, vol. 38, no. 3, pp. 689–706, 2023.
- [42] F. Fantin, A. Mattocks, C. J. Bulpitt, W. Banya, and R. Chakravarthi, “Is augmentation index a good measure of vascular stiffness in the elderly?,” *Age and Ageing*, vol. 36, no. 1, pp. 43–48, 2006.
- [43] B. Harbaoui, P.-Y. Courand, A. Cividjian, and P. Lantelme, “Development of coronary pulse wave velocity: new pathophysiological insight into coronary artery disease,” *Journal of the American Heart Association*, vol. 6, no. 2, p. e004981, 2017.
- [44] “Arterial pressure waveforms,” in *Cardiovascular Physiology*, pp. 150–152, 2022.
- [45] M. Böhmer, J.-C. Reil, P. Deedwania, J. B. Kim, and J. S. Borer, “Resting heart rate: risk indicator and emerging risk factor in cardiovascular disease,” *The American Journal of Medicine*, vol. 128, no. 3, pp. 219–228, 2015.
- [46] N. Paradkar and S. R. Chowdhury, “Cardiac arrhythmia detection using photoplethysmography,” in *2017 39th Annual International Conference of the IEEE Engineering in Medicine and Biology Society (EMBC)*, pp. 113–116, IEEE, 2017.
- [47] A. C. Flint, C. Conell, X. Ren, N. M. Banki, S. L. Chan, V. A. Rao, R. B. Melles, and D. L. Bhatt, “Effect of systolic and diastolic blood pressure on cardiovascular outcomes,” *New England Journal of Medicine*, vol. 381, no. 3, pp. 243–251, 2019.
- [48] J. M. Nolde, L. M. Lugo-Gavidia, D. Kannenkeril, J. Chan, S. Robinson, A. Jose, A. Joyson, L. Schlaich, R. Carnagarin, O. Azzam, *et al.*, “Simultaneously measured inter-arm blood pressure difference is not associated with pulse wave velocity in a clinical dataset of at-risk hypertensive patients,” *Journal of Human Hypertension*, vol. 36, no. 9, pp. 811–818, 2022.
- [49] Y. Liang, Z. Chen, G. Liu, and M. Elgendi, “A new, short-recorded photoplethysmogram dataset for blood pressure monitoring in china,” *Scientific Data*, vol. 5, no. 1, pp. 1–7, 2018.
- [50] M. A. Pimentel, A. E. Johnson, P. H. Charlton, D. Birrenkott, P. J. Watkinson, L. Tarassenko, and D. A. Clifton, “Toward a robust estimation of respiratory rate from pulse oximeters,” *IEEE Transactions on Biomedical Engineering*, vol. 64, no. 8, pp. 1914–1923, 2016.
- [51] G. Li, K. Watanabe, H. Anzai, X. Song, A. Qiao, and M. Ohta, “Pulse-wave-pattern classification with a convolutional neural network,” *Scientific Reports*, vol. 9, no. 1, p. 14930, 2019.



**Sahar Waqar** was born in Lahore, Pakistan in 1992. She received the B.Sc CE degree from the CE Department in June 2014 and Masters in CS in April 2017. She is currently a PhD scholar in CS Dept., UET Lahore Pakistan since Sep 2019. She has also completed four year degree of Fazil-e-Tibb-wal-Jarahat (FTJ) i.e., Diploma in Unani Medical System and Surgery (DUMS) in 2021. from same university. From 2014-2016, she was working as a Software Engineering in Techlogix. After

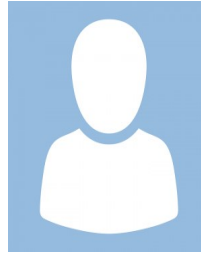
that, she worked as a RESEARCH OFFICER and TEAM LEAD in Computer Vision and Machine Learning Lab, Al-Khawarizmi Institute

of Computer Science (KICS) for one year (2016-2017). Since 2017, she is working as a LECTURER in CE Dept., UET Lahore Pakistan. Currently, her research interests includes processing of health care related information from non-invasive sensors.

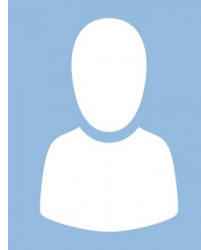


**Samyan Qayyum** was born in Narowal, Pakistan. He received the B.Sc CS degree from UET Lahore in June 2014 and Masters in CS in April 2017. His Work experience includes Full Stack Software Development with different software companies and as Research Team Lead in Computer Vision and Machine Learning Lab. He is currently a PhD scholar in CS Dept., UET Lahore Pakistan and Lecturer in the same department. He has also completed four year degree of Fazil-e-Tibb-

wal-Jarahat (FTJ) i.e., Diploma in Unani Medical System and Surgery (DUMS) in 2021. His research interests include machine learning, Computer Vision and Deep Learning.



**Anam Mukhtar** received the B.S. degrees in CE from Dept. of CE, UET Lahore Pakistan. She is currently working as Software Quality Assurance Engineer at Uppgenics international.



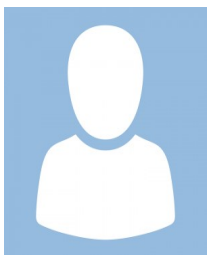
**Rimsha Shahzad** received the B.S. degrees in CE from Dept. of CE, UET Lahore Pakistan. She is currently enrolled as M.S. student is Dept. of CS in the same university.



**Talha Waheed** received the B.S. degree in the CS from National University of Computer and Emerging Sciences. After that, he received his PhD degree in CS from UET Lahore Pakistan. He has also completed four year degree of Fazile-Tibb-wal-Jarahat (FTJ) i.e., Diploma in Unani Medical System and Surgery (DUMS). He is currently serving as Assistant Professor in Dept. of CS, UET Lahore Pakistan. His research interests include the knowledge representation in Unani Medicines.



**Ahmed Shahid** received the B.S. degrees in CE from Dept. of CE, UET Lahore Pakistan. He is currently working as a Software Engineer in Confiz Pakistan.



**Amna Munir** received the B.S. degrees in the CE from Dept. of CE, UET Lahore Pakistan.